Using a Cell-to-ECG Model to Evaluate Ischemia Detection from Different Lead Sets

WH Gao[1], Y Chen[1], XD Han[1], P Zhu[1], JQ Xue[2]

[1]GE Research, Shanghai, China
[2]GE Healthcare, Wauwatosa, WI, USA

Abstract

In this study, we designed a Cell-to-ECG forward model to simulate ischemia condition from cell level, and then defined five different ischemia locations including inferior, anterior, septal, lateral, and apex on an actual 3-D heart geometry from CT images. For simulating the early ischemia, the ion channels are adjusted through concentration and conductance. The extent of ischemia is defined with a ten-layer model from endocardial to epicardial. The model can generate ECG signal from any position on the torso, therefore different lead sets can be configured based on the selected subset from the torso. All reduced lead sets are converted to 12-lead ECGs by published conversion matrixes. The criteria of acute ischemia detection are based on AHA/ACC recommendation of 2 contiguous leads 200 uV ST elevation for chest leads, and 100 uV ST elevation for limb leads. The model reveals the consistent ECG pattern with the accepted criteria, especially the reciprocal ST changes from the simulated transmural ischemia cases. The reduced lead sets show comparable detection accuracy and sensitivity to the standard 12-lead for most ischemia locations except for anterior MI, where more specific criteria can adapt to the changes of the ECG morphology from reduced lead sets.

1. Introduction

Multi-lead ECG for ischemia detection and monitoring is still one of the most time sensitive techniques despite rapid development of other image modalities. At the meantime, using fewer electrodes in those long-term monitoring situation is preferred for the reasons of patient comfort, noise reduction and limit of transmission bandwidth. Over the years, several popular methods of interpolating from reduced lead set to standard 12-lead set have been proposed and implemented in various cardiac instruments [1-3].

There are mainly 2 types of usage for the reduced lead set ECG. One is for long term monitoring, and the other is for a single 10-second ECG interpretation. In the case of long-term monitoring purpose, relative morphology changes could be more important. Whereas for the single 10-second ECG interpretation, the closeness of the ECG patterns based on the reduced lead set to those of standard 12-lead becomes more important, since in most situations, the criteria based on standard 12-lead set is used for the reduced lead set. In both types of usage, we all need to know how ECG patterns change when reduced lead sets are used, and if the changes would affect sensitivity or specificity for the interpretations. In this study, we focused on acute ischemia interpretations. One method for the evaluation of effectiveness of reduced lead sets is to sample large number ECGs from both standard lead sets and reduced lead sets with confirmed interpretations, preferably by other methods other than ECGs, for example, cardiac enzyme tests. The other method is using a modeling approach, through which ischemia in different heart locations with different severities can be simulated and ECGs can be generated for all possible lead configurations. The model generated ECGs, based on both standard and reduced lead sets, can be compared based on different interpretation criteria.

Over the years, there have been quite a few research activities around heart modeling, both forward and inverse models [4-7]. These models can be divided into two categories, according to whether a cellular-level model involved in the high level model as a discrete set of cells or as a continuum.

In the continuum-style involvement, the whole heart simulation is formulated as the solving of partial-differential equations. Due to the sharp rise in action potential, converged numerical implementations simulating normal activity require smaller steps and finer spatial resolution, which usually need large amount of computation works.

In the current discrete-style involvement, heart is subdivided into dozens of regions (normally less than 100) and for each region an equivalent dipole is determined by combining the individual effect of the cell sets inside. Each cell set is initially specified a parameterized action profile, in which the sharp rise starts from the beginning. Then the rise is shifted according to the acquired depolarization-time isochrones. To calculate

the cardiac electrical field, the resultant dipoles are assumed to act at the region centroids and used to compute the BSPM. An advantage of this approach is the fast simulation speed due to the lower amount of computation compared with the first approach. However the parameterized action profiles and the equivalent dipoles decrease the fidelity of the model, both at the cellular level and at the organic level.

The model we proposed here belongs to the second case but with some major modifications. The first modification is the determination of cellular action profiles for the cell sets. Instead of using a parameterized action profile (defined by action potential duration (APD), peak amplitude etc.), we adopt ordinary-differential-equation (ODE) type ion channel models; so that the effect of MI on heart can be modeled by changing the ion-channel parameters. The second characteristic is the application of a bidomain model based FEM-BEM coupling formulation in the cardiac electric field [5]. The heart domain is discretized by tetrahedron mesh and FEM formulation is taken for it. The anisotropy of myocardium conductivity can be part of model by setting conductivity tensor for each FEM node [6,7]. In this way, myocardium anisotropy can be also included into the model.

2. Methods

2.1. Cell-to-ECG model

The PB model [8] is used as the base for the human cardiac cell modeling. To make best of variable-step numerical integration technique to attain high computational efficiency, we replace the intracellular calcium dynamic module in PB model with the much simpler one in TNNP model [9]. With this alteration, CVODE integrator is used to calculate the action potential. Moreover, the ATP-dependent K^+ current ($I_{K,ATP}$) was incorporated into this model using Shaw-Rudy's formulation [10, 11] for ischemia and infarction simulation.

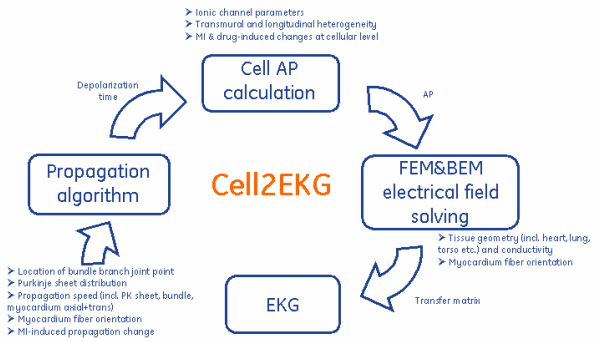

Figure 1. Flowchart of the Cell-to-EKG modeling

A bidomain model based FEM-BEM coupling formulation in the cardiac electric field is developed [5]. Figure 1 illustrates the system configuration of our model. The governing equations are given as following:

$$\nabla \cdot \kappa_{myo} \nabla \varphi_{myo}(r) = -\nabla \cdot \sigma_{myo} \nabla V_{myo}(r), \quad \forall r \in \Omega_{myo} \quad (1)$$

$$\nabla \cdot \kappa_{blood} \nabla \varphi_{blood}(r) = 0, \quad \forall r \in \Omega_{blood} \quad (2)$$

$$\nabla \cdot \kappa_{lung} \nabla \varphi_{lung}(r) = 0, \quad \forall r \in \Omega_{lung} \quad (3)$$

$$\nabla \cdot \kappa_{torso} \nabla \varphi_{torso}(r) = 0, \quad \forall r \in \Omega_{torso} \quad (4)$$

2.2. Define ischemia zone

The definition of ischemia area is based on the original left ventricular segmentation proposed by Sylvester [12], as shown in Figure 3. There are total 17 zones in this definition, which were then registered with the 3-D heart geometry model based on our CT images.

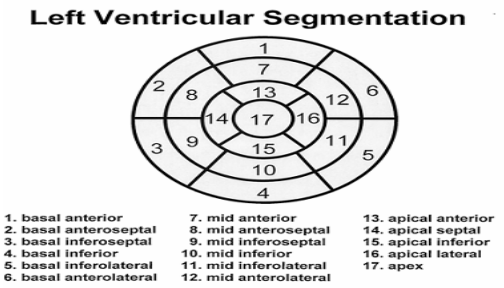

Figure 2. The diagram of left ventricular segmentation with 17 zones.

2.3. Define ischemia cell parameters

Two degrees of early acute ischemia were considered in this study as *stages 1*, *2*. Different from the definition in [11] which associates the ischemia stages with the time after acute global ischemia, the stages in this study are assigned with decreasing gradients at plateau of action potential and increasing gradients in resting potentials. The major parameter setting is shown in Table 1. Figure 3 depicts the typical action potentials at the two stages.

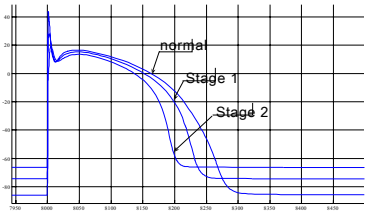

Figure 3. Action potentials corresponding to different ischemia stages

2.4. Reduced lead set

The reduced lead set 12RL is a subset of the standard

12-lead, consisting of all the limb leads and precordial lead v1 and v5 [1]. Another 4 precordial leads are derived from lead I, II, v1 and v5 [13].

Table 1 Parameter settings for the key ion channels and conductance

	Normal	Ischemia Stage 1	Ischemia Stage 2
$[K^+]_o$ mmol/L	5.4	8	14
I_{na} conductance	100%	75%	45%
I_{caL} conductance	100%	75%	45%
$[ATP]_i$ mmol/L	6.8	5.7	3.5

2.5. Ischemia detection from ECGs

The criteria for acute ischemia detection are based on ACC/AHA recommendation. i.e. two contiguous leads ST segment elevation larger than 200 uV for precordial leads and 100uV for limb leads. An intermediate ST elevation is defined by smaller threshold as shown below. The ST value is measured at the 80 msec after J point. Following are the symbols used for ST elevation and ST depression.

- ++: greater than 200uV in V leads and 100uV in the extremity leads
- +: greater than 150uV but smaller than 200uV in V leads or greater than 75uV but smaller than 100uV in the extremity leads
- --: smaller than -200uV in V leads and -100uV in the extremity leads
- -: smaller than -150uV but greater than –200uV in at V leads or smaller than -75uV but greater than –100uV in the extremity leads

3. Results

3.1. Simulation examples

As an example, Figure 4 displays the simulated anterior-lateral MI and baseline 12-lead ECGs, its area in the left ventricle diagram, and its position in the 3-D heart model. We can see that the ST levels are elevated in anterior and lateral leads and depressed in inferior leads. Figure 5 displays the similar diagrams for inferior MI.

3.2. Detection result

Based on the methods described above, both standard 12-lead and the reduce 12-lead ECGs are generated for normal and five different localized MIs: Anterior, Septal, Lateral, Inferior, and Apex. Two stages of MI were generated for all locations. The criteria described previously are used to mark the detection results in the tables, where Table 2 describes the results for standard 12-lead, and Table 3 is for the reduced lead.

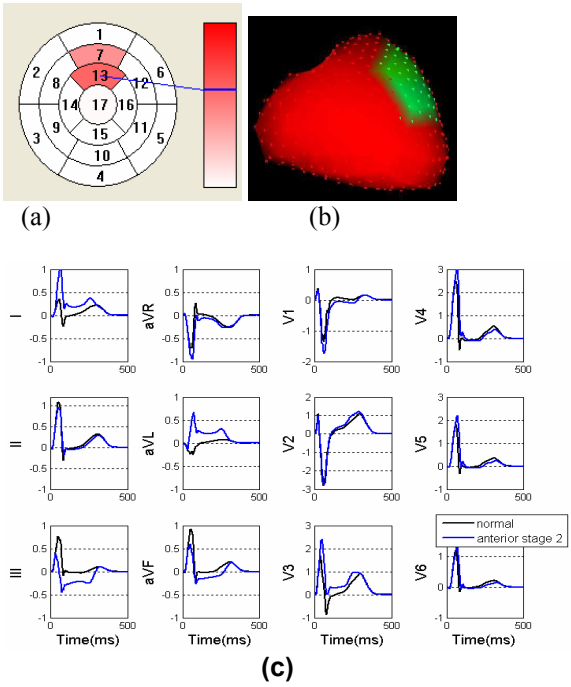

Figure 4. Simulated anterior MI (a) areas in the left ventricle diagram, (b) corresponding position in the 3-D heart model, (c) ECGs generated from the model.

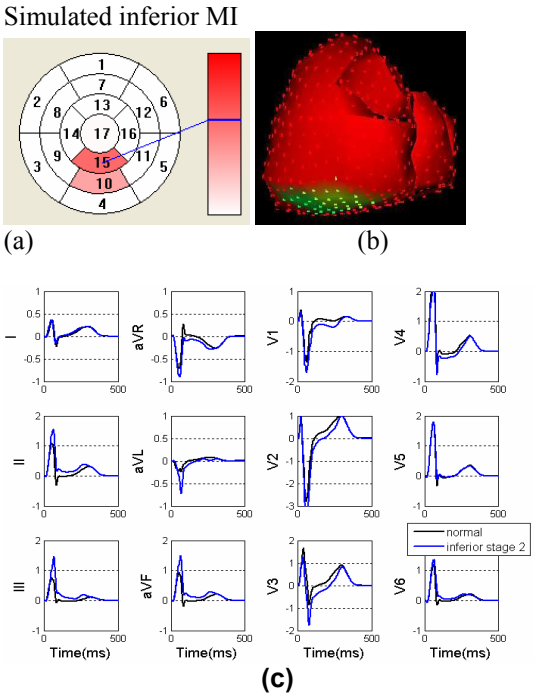

Figure 5. Simulated inferior MI (a) areas in the left ventricle diagram, (b) corresponding position in the 3-D heart model, (c) ECGs generated from the model.

It can be seen, from Table 1, that standard 12-lead ECG can detect simulated MI in all locations, and is most sensitive to anterior, inferior, and apex MI, where MI in stage 1 can be detected.

Table 3 shows that for the reduced lead set, the sensitivity is good for inferior and apex MI. For other locations, its sensitivity is generally lower than that of standard 12-lead, especially for anterior MI.

It also shown that reciprocal ST depressions are present for most MI locations in both lead sets.

Table 2. Transmural Ischemia detection Based on Standard 12-lead

	Normal	Anterior (lateral)		Septal		Lateral		Inferior		Apex	
Ischemic stage		Stage 1	Stage 2	Stage 1	Stage 2	Stage 1	Stage 2	Stage 1	Stage 2	Stage 1	Stage 2
I	0	+	++	0	0	++	++	0	0	0	+
II	0	0	0	0	0	0	0	++	++	++	++
III	0	--	--	0	0	0	--	++	++	0	++
aVR	0	0	-	0	0	-	--	0	--	-	--
aVL	0	++	++	0	0	+	++	0	-	0	0
aVF	0	0	--	0	0	0	0	++	++	+	++
V1	0	0	0	0	+	0	0	0	-	0	0
V2	0	++	++	++	++	0	0	0	--	0	0
V3	0	++	++	0	0	0	0	0	--	++	++
V4	0	0	0	0	0	0	0	0	-	++	++
V5	0	0	0	0	0	0	++	0	0	++	++
V6	0	0	0	0	0	0	++	0	0	0	++

Table 3. Transmural Ischemia detection based on Sub-12-lead (all limb leads + v1, v5)

	Normal	Anterior (lateral)		Septal		Lateral		Inferior		Apex	
Ischemic stage		Stage 1	Stage 2	Stage 1	Stage 2	Stage 1	Stage 2	Stage 1	Stage 2	Stage 1	Stage 2
I	0	+	++	0	0	++	++	0	0	0	+
II	0	0	0	0	0	0	0	++	++	++	++
III	0	--	--	0	0	0	--	++	++	0	++
aVR	0	0	-	0	0	-	--	0	--	-	--
aVL	0	++	++	0	0	+	++	0	-	0	0
aVF	0	0	--	0	0	0	0	++	++	+	++
V1	0	0	0	0	+	0	0	0	-	0	0
V2	0	0	0	0	+	0	0	0	--	0	0
V3	0	0	0	0	0	0	+	0	0	+	++
V4	0	0	0	0	0	+	++	0	0	++	++
V5	0	0	0	0	0	0	++	0	0	++	++
V6	0	0	0	0	0	0	++	0	0	+	++

4. Discussion and conclusions

The modeling approach reveals the consistent ECG patterns with the accepted criteria, especially the reciprocal ST changes from the simulated transmural ischemia cases. The reduced lead sets show comparable detection accuracy and sensitivity to the standard 12-lead for most ischemia locations except for anterior MI, where lower threshold need to be used.

Our experiment showed that despite some ECG morphology difference between reduced lead set and standard 12-lead, the sensitivity and specificity of ischemia detection based on the reduced lead set are close to those of standard 12-lead. The only exception is anterior acute MI, where reduced lead sets have higher false negative rate if following ACC/AHA guideline. However, the experiments carried in actual sampled ECGs showed the specifically trained criteria can adapt to the morphology change and improve the sensitivity significantly for acute anterior MI cases [13].

The modeling approach used in this study can also be extended to evaluation of other reduced lead sets.

References

[1] Drew BJ, et al. Comparison of a new reduced lead set ECG with the standard ECG for diagnosing cardiac arrhythmias and myocardial ischemia. J Electrocardiol. 2002;35 Suppl:13-21.

[2] Nelwan SP, et al. Reconstruction of the 12-lead electrocardiogram from reduced lead sets. J Electrocardiol. 2004 Jan;37(1):11-8.

[3] Rautaharju PM, et al. Comparability of 12-lead ECGs derived from EASI leads with standard 12-lead ECGS in the classification of acute myocardial ischemia and old myocardial infarction.J Electrocardiol.2002;35 Suppl:35-9

[4] Lorange M. and Gulrajani R. M. A computer heart model incorporating anisotropic propagation: I. Model construction and simulation of normal activation. J. Electrocardiol 1993; 26, 245-261

[5] Fischer G., et al.. A bidomain model based BEM-FEM coupling formulation for anisotropic cardiac tissue. Annals of Biomedical Engineering, 2000; 28, 1229-1243

[6] Roth B. J. Electrical conductivity values used with the bidomain model of cardiac tissue. IEEE Trans. Biomed. Eng., 1997; 44: 326-28

[7] Sachse F. B., et al. Modeling of fiber orientation in the ventricular myocardium with MR diffusion imaging. Proc. Computers in Cardiology, 2001; 28: 617-620

[8] Priebe L, et al. Simulation study of cellular electric properties in heart failure. Circ. Res. 1998; 82; 1206-1223

[9] Ten Tusscher K H W J, et al. A model for human ventricular tissue Am. J. Physiol. Heart Circ. Physiol, 2004; 286; H1573–89

[10] Shaw RM, et al. Electrophysiologic effects of acute myocardial ischemia: a theoretical study of altered cell excitability and action potential duration. Cardiovascular Research, 1997; 35; 256-272

[11] Rodrı´guez B, et al. Effect of acute global ischemia on the upper limit of vulnerability: a simulation study. Am. J. Physiol. Heart Circ Physio. 2004; 286, H2078-H2088

[12] Cerqueira M, et al. Standardized myocardial segmentation and nomenclature for tomographic imaging of the heart : a statement for healthcare professionals from the Cardiac Imaging Committee of the Council on Clinical Cardiology of the American Heart Association. Circulation. 2002; 105: 539-542

[13] Xue JQ, Adapting ECG morphology changes from reduced-lead set by specifically trained algorithms for acute ischemia detection, Computer in Cardiology 2007

Address for correspondence
Joel Xue
9900 Innovation Drive
Wauwatosa, WI 53226, USA